

Are your **MRI contrast agents** cost-effective?

Learn more about generic **Gadolinium-Based Contrast Agents**.



**FRESENIUS
KABI**

caring for life

AJNR

Cervical Cordotomy for Intractable Pain: Do Postoperative Imaging Features Correlate with Pain Outcomes and Mirror Pain?

A. Berger, M. Artzi, O. Aizenstein, T. Gonen, R. Tellem, U. Hochberg, D. Ben-Bashat and I. Strauss

This information is current as of May 11, 2024.

AJNR Am J Neuroradiol 2021, 42 (4) 794-800

doi: <https://doi.org/10.3174/ajnr.A6999>

<http://www.ajnr.org/content/42/4/794>

Cervical Cordotomy for Intractable Pain: Do Postoperative Imaging Features Correlate with Pain Outcomes and Mirror Pain?

 A. Berger,  M. Artzi,  O. Aizenstein,  T. Gonen,  R. Tellem,  U. Hochberg,  D. Ben-Bashat, and  I. Strauss



ABSTRACT

BACKGROUND AND PURPOSE: Percutaneous cervical cordotomy offers relief of unilateral intractable oncologic pain. We aimed to find anatomic and postoperative imaging features that may correlate with clinical outcomes, including pain relief and postoperative contralateral pain.

MATERIALS AND METHODS: We prospectively followed 15 patients with cancer who underwent cervical cordotomy for intractable pain during 2018 and 2019 and underwent preoperative and up to 1-month postoperative cervical MR imaging. Lesion volume and diameter were measured on T2-weighted imaging and diffusion tensor imaging (DTI). Lesion mean diffusivity and fractional anisotropy values were extracted. Pain improvement up to 1 month after surgery was assessed by the Numeric Rating Scale and Brief Pain Inventory.

RESULTS: All patients reported pain relief from 8 (7–10) to 0 (0–4) immediately after surgery ($P = .001$), and 5 patients (33%) developed contralateral pain. The minimal percentages of the cord lesion volume required for pain relief were 10.0% on T2-weighted imaging and 6.2% on DTI. Smaller lesions on DWI correlated with pain improvement on the Brief Pain Inventory scale ($r = 0.705$, $P = .023$). Mean diffusivity and fractional anisotropy were significantly lower in the ablated tissue than contralateral nonlesioned tissue ($P = .003$ and $P = .001$, respectively), compatible with acute-phase tissue changes after injury. Minimal postoperative mean diffusivity values correlated with an improvement of Brief Pain Inventory severity scores ($r = -0.821$, $P = .004$). The average lesion mean diffusivity was lower among patients with postoperative contralateral pain ($P = .037$).

CONCLUSIONS: Although a minimal ablation size is required during cordotomy, larger lesions do not indicate better outcomes. DWI metrics changes represent tissue damage after ablation and may correlate with pain outcomes.

ABBREVIATIONS BPI = Brief Pain Inventory; FA = fractional anisotropy; MD = mean diffusivity; RF = radiofrequency; NRS = Numeric Rating Scale; STT = spinothalamic tract; POD = postoperative day

Percutaneous cervical cordotomy is used to selectively disconnect the nociceptive spinothalamic fibers traveling in the anterolateral quadrant of the spinal cord.¹ It offers relief for patients with unilateral intractable oncologic pain below the C4 dermatome level who have failed conservative treatment.² Success rates in contemporary series reach nearly 80% with advancing technology, including combined intraoperative CT guidance and radiofrequency (RF)

tools.^{3–5} The 2 main reasons for patient dissatisfaction from the procedure include failure in achieving complete and long-standing pain relief (up to 20%) and the development of postoperative pain in the contralateral side (at least 17%).^{6–8}

Previous studies showed that a lesion of at least 20% of the entire cord and localized in the anterolateral quadrant is necessary to achieve effective pain relief, yet no clear correlation was found between the size of the lesion and the degree of improvement.^{9–11} More recent MR imaging- and DWI-based studies found direct correlations between the degree of the lesion's mean diffusivity (MD) as a measurement of local neural damage and improvement on pain assessment scores after surgery.¹² However, data on the mechanisms behind the postoperative contralateral pain phenomenon and its predicting factors are still lacking.


We performed this prospective study to analyze potential correlations between clinical responses to surgery, including pain relief and contralateral pain with several postoperative MR imaging-based parameters, such as the size of the lesions and their

Received August 6, 2020; accepted after revision October 28.

From the Department of Neurosurgery (A.B., I.S.); Sagol Brain Institute (M.A., T.G., D.B.-B.); Department of Radiology (O.A.), The Palliative Care Service (R.T.); Institute of Pain Medicine (U.H.); Division of Anesthesiology, Tel Aviv Medical Center (U.H.), Tel Aviv, Israel; and Sackler School of Medicine (A.B., M.A., O.A., T.G., R.T., U.H., D.B.-B., I.S.), Tel Aviv University, Tel Aviv, Israel.

A. Berger and M. Artzi contributed equally to the manuscript.

Please address correspondence to Assaf Berger, MD, Department of Neurosurgery, Tel Aviv Medical Center, 6 Weizmann St, Tel Aviv, Israel 6423906; e-mail: assaf.berger@gmail.com

 Indicates article with online supplemental data.

<http://dx.doi.org/10.3174/ajnr.A6999>

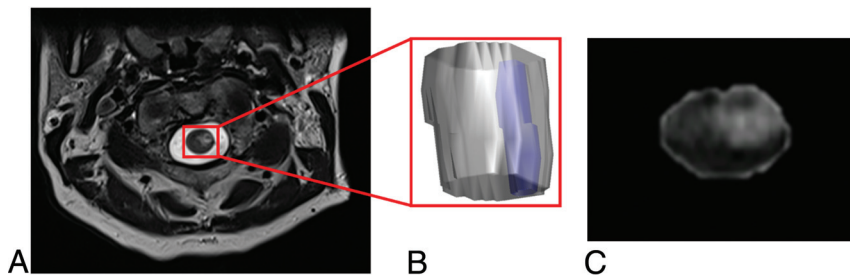


FIG 1. Manual-based segmentation of the hyperintense lesion area (*blue*) and the spinal cord that delineates it (*gray*) based on T2-weighted imaging.

DWI metrics, including trace, MD, and fractional anisotropy (FA) measurements.

METHODS

Demographic and Clinical Parameters

We prospectively collected data of patients with intractable oncologic pain who underwent cordotomy in our center during 2018 and 2019, focusing on the following parameters: age, sex, cancer type, original pain side, location, and duration before surgery. All patients who signed informed consent and underwent pre- and postoperative MR imaging were included in the study. Their data were recorded throughout their course of treatment and follow-up period, and they are reported in this article. We also reviewed oncologic imaging work-ups to seek lesions that were considered nonpainful before surgery and that were located along the midline (spine or pelvis) or contralateral to the original painful side.

Patients were asked to fill in pain assessment questionnaires before and after surgery, including the Numeric Rating Scale (NRS) and Brief Pain Inventory (BPI) scores. NRS is used to evaluate the average degree of pain as it is currently being experienced. The BPI score has been validated for patients with cancer, and it estimates several aspects of the magnitude of pain outcomes over a longer time period.¹³ We measured the relative decrease in BPI severity score after surgery and present the results as the percentage of decrease from the preoperative BPI severity score.

Surgical Technique

Our surgical technique has been previously described.³ In short, the procedure requires cooperation of the patient for electrophysiologic verification of the spinothalamic tract (STT), usually with mild sedation (remifentanyl and propofol) during the initial needle insertion until dural puncture. Patients are first injected with 8 mL of intrathecal iohexol contrast dye (Omnipaque 300 mg/mL) by means of either lumbar puncture or direct cervical injection. We then use O-arm lateral fluoroscopy to insert the needle into the lateral C1–C2 interspace. Needle location and trajectory are verified with CT. After the correct angle is achieved, an RF electrode is introduced through the cannula and slowly advanced while the impedance is monitored. When the cord has been penetrated as indicated by an increase in impedance, we perform another CT scan to verify the anatomic position of the electrode. Then electrophysiologic monitoring testing with both motor and

sensory stimulation is used to confirm proper electrode location inside the spinothalamic tract. After this has been accomplished, a test lesion is created at 60° for 30 seconds while simultaneously monitoring motor strength. A permanent lesion is then created at 80° for 60 seconds. If the painful area is not completely covered, additional lesions are often created in the same manner after gentle repositioning of the electrode until satisfactory pain relief is achieved. The procedure usually involves more than 1 pial penetration (median, 4;

range, 2–10) to find the optimal target and usually more than 1 ablation to achieve satisfactory pain relief (median, 3; range, 2–5). The electrode is repositioned either anteroposteriorly or mediolaterally, according to the findings of intraoperative stimulation. The STT is organized in the cervical spinal cord with the fibers from the leg located posterolaterally and fibers from the hand and shoulder located more anteromedially.

Imaging

Patients underwent MR imaging of the cervical spine before and again 1–2 days after the procedure ($n = 15$). They were also scheduled to undergo an MR imaging 1 month after surgery, but only 5 of them were able to do so because of the complexity of their condition. Scans were performed on a 3T MR imaging scanner (Magnetom Prisma; Siemens) and included axial turbo spin-echo T2-weighted imaging with TR of 5080 ms, echo time TE of 90 ms, and voxel dimensions of $0.56 \times 0.56 \times 3.3 \text{ mm}^3$. Also included was diffusion tensor imaging (DTI) acquired with TR of 10,000 ms, TE of 69 ms, with 24 gradient directions, b-values of $0,1000 \text{ s/mm}^2$, and voxel dimensions of $0.65 \times 0.65 \times 3 \text{ mm}^3$. Transverse slices were set to cover the C1–C7 vertebral levels. To minimize possible deviations between pre- and postoperative MR imaging that might result from differences in angulation of the axial slices or orientation of the neck, examinations were performed by the same technician and in the same clinical setting.

Image Analysis

Imaging analysis was performed using FMRIB Software Library (<http://www.fmrib.ox.ac.uk/fsl>) and Analyze (version 11.0; AnalyzeDirect) software. It included manual-based segmentation of the hyperintense lesion area and the spinal cord that delineates it by means of AnalyzeDirect separately for the T2-weighted imaging (Fig 1) and diffusion trace images. Segmentation was performed on axial images using a semiautomatic threshold-based algorithm (region of interest module). Segmentation was initiated by manually setting a seed point at the hyperintense lesion area or at the lesioned cord on the trace image and manually adapting the threshold range. Semiautomatic segmentation of the region of interest by means of a threshold-based algorithm instead of manual segmentation is expected to minimize the effects of partial volume averaging. The following numeric parameters were extracted based on the extracted lesion area: lesion volume (in cc), lesion-to-cord ratio (in percentages) at the level

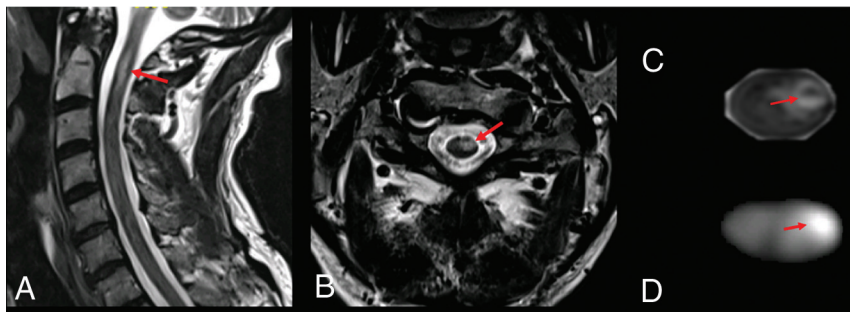


FIG 2. Postoperative MR imaging findings 1 day after cervical cordotomy. *Red arrows* indicate the cordotomy ablation. *A*, Sagittal T2-weighted imaging. *B*, Axial T2-weighted imaging. *C* and *D*, Axial diffusion trace images.

of ablation, and largest in-plane axial (minor axis) and sagittal (major axis) lengths (in millimeters).

Last, we measured the minimal, maximal, and average MD and FA values of the lesions' DWI areas (Fig 2) and of the non-lesioned cord as measured contralateral to the side of the lesion on postoperative DTI. In addition, we measured preoperative MD and FA on DTI of the future lesion's area on the same anatomic cervical segment.

Statistical Analysis

Statistical procedures were performed with SPSS 21.0 software (IBM).

Categorical characteristics of patients with and without postoperative contralateral pain were compared using the Fisher exact test. Comparison of continuous variables between unrelated samples was performed using the Mann-Whitney U test, and the Wilcoxon test was used for related samples. Correlations between continuous study parameters were performed with the Spearman correlation. Analyses were performed by nonparametric tests because of the small sample size and the fact that several parameters did not show normal distribution on normality tests. A P value $<.05$ (2-sided) was considered statistically significant.

This study was approved by the institutional review board.

RESULTS

Clinical and Demographic Data

Twenty patients with cancer underwent percutaneous cervical cordotomy as part of a prospective trial in our center between February 2018 and July 2019. Five patients were excluded from this study because they could not undergo preoperative MR imaging because of pain or general fatigue. The mean age of our study population was 65 ± 9 years. The Online Supplemental Data describe individual demographic, clinical, and imaging parameters of the study group. All 15 patients had localized unilateral intractable pain. The average duration of pain before surgery was 10 ± 7 months. Four patients (27%) had pain in the upper extremities and 11 in the lower part of the body (73%). Most patients mainly had tumor-associated nociceptive pain, but 1 patient with sciatic malignant peripheral nerve sheath tumor also had painful plexopathy. One patient died from a general deterioration associated with his primary disease within 1 month after

surgery; therefore, only relatively short-term postoperative data are available for that patient.

Imaging Data

All lesions were hyperintense on T2-weighted imaging sequences with an average volume of 0.28 ± 0.13 cc and $19\% \pm 8\%$ of the total cord volume at the level of ablation. Lesions on diffusion trace images were smaller and measured 0.08 ± 0.05 cc and $15\% \pm 9\%$ of the total cord volume at the same level. The average percentages of the lesioned cross-sectional area of the cord on T2-weighted imaging and diffusion trace

images were $24\% \pm 8\%$ and $26\% \pm 8\%$, respectively. The mean major axis (sagittal) length on T2-weighted imaging and trace images was 15 ± 1.8 mm and 7.6 ± 1.8 mm, respectively.

The average MD and FA of the measured lesions were $0.905 \pm 0.216 \cdot 10^{-3}$ mm²/s and 0.406 ± 0.07 a.u. (arbitrary unit), respectively (Online Supplemental Data).

Clinical Outcomes and Imaging Correlations

All 20 patients reported a substantial improvement in the original pain intensity immediately after surgery: the median preoperative NRS was 8 (range 7–10) compared with the postoperative NRS of 0 (0–4) ($P = .001$). One month after surgery, 1/14 surviving patients had pain in the original distribution of a similar intensity as the preoperative levels. The other 13 patients reported a complete or near-complete resolution of the original pain.

The average percentages of the ablated cord's cross-sectional area were $22.1\% \pm 7.6\%$ and $26.4\% \pm 8.0\%$ on the T2-weighted imaging and diffusion trace images, respectively, for the group of patients who survived 1 month after surgery. The minimal lesion volumes that achieved adequate pain response were 13.4% and 9.6% for T2-weighted imaging and the diffusion trace images, respectively. The average volumes of the lesioned cord on the T2-weighted imaging and diffusion images were 0.3 ± 0.1 cc and 0.1 ± 0.05 cc, which respectively included $17.8\% \pm 6.9\%$ and $14.4\% \pm 8.3\%$ of the cord's volume at the ablated segments. The minimal volumes were 0.15 cc and 0.03 cc, including 10.0% and 6.2% of the cord's volume on T2-weighted imaging and diffusion images, respectively. No significant differences were noted in the degree of 1-month postoperative decrease in NRS when comparing patients with ablation below or above 20% of the cord's T2-weighted imaging cross-sectional area (8 ± 1 , $n = 5$ and 8 ± 3 , $n = 9$, respectively; $P = .518$). Similarly, no significant differences between the groups were noted when diffusion was used ($P = .635$).

Ten patients completed BPI questionnaires and reported a significant improvement in pain severity scores, from 28 ± 6 before surgery to 18 ± 13 at 1 month after surgery ($P = .022$). We measured the relative decrease in the BPI severity score after surgery as the percentage of decrease from the preoperative BPI severity score. There was a correlation between the minor axis (in-plane, axial) length of the lesion on diffusion trace images and the change in BPI severity score ($r = 0.827$, $P = .003$); the

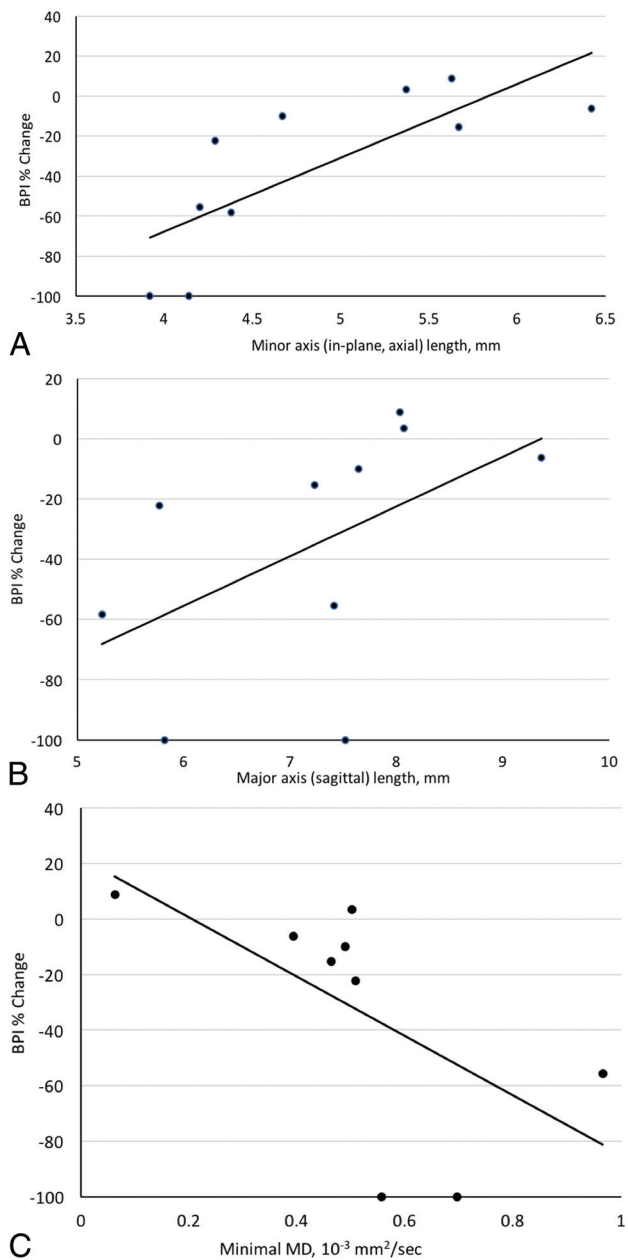


FIG 3. Spearman correlation between percentage of change in BPI 1 month after cordotomy and the following values: A, Ablation size of minor axis (in-plane, axial) on diffusion trace images, ($r = 0.827$, $P = .003$). B, Major axis (sagittal) length on diffusion trace images ($r = 0.705$, $P = .023$). C, Lesion minimal MD, $10^{-3} \text{ mm}^2/\text{s}$ ($r = -0.821$, $P = .004$).

shorter the lesion, the greater was the relative (percent) decrease in BPI severity score after surgery. Similarly, a possible correlation was demonstrated between the change in BPI severity and the major axis (sagittal) length of the lesion on diffusion trace images ($r = 0.705$, $P = .023$) (Fig 3).

In addition, we evaluated the correlation between the size of the lesion on the postoperative MR imaging and the number of pial penetrations and the number of ablations during surgery. The results showed a significant correlation between the major axis (sagittal) length of the lesion on T2-weighted imaging and

Table 1: Change in BPI after cordotomy and its correlation with different postoperative imaging characteristics

% BPI Change Correlation (n = 10/15)	Spearman Rho	Significance (2-Tailed)
T2-weighted imaging total cord, %	-0.091	.802
Diffusion, total cord, %	0.590	.073
Major axis (sagittal), T2-weighted imaging, mm	-0.529	.116
Minor axis (in-plane, axial), T2-weighted imaging, mm	-0.091	.802
Major axis (sagittal), DWI, mm	0.705	.023
Minor axis (in-plane, axial), DWI, mm	0.827	.003
Minimal MD	-0.821	.004
Maximal MD	-0.091	.802
Average MD	-0.450	.192
Minimal FA	-0.148	.688
Maximal FA	0.255	.476
Average FA	0.292	.413

the number of penetrations ($r = 0.566$, $P = .028$). There were no additional significant correlations between any of the other imaging parameters and the number of pial penetrations or ablations.

Furthermore, we measured each lesion's minimal, maximal, and average MD and FA on the pre- and postoperative DTI studies. The postoperative MD was significantly lower at the site of the lesion compared with the preoperative MD values of the same area ($0.947 \pm 0.213 \times 10^{-3} \text{ mm}^2/\text{s}$ and $1.125 \pm 0.304 \times 10^{-3} \text{ mm}^2/\text{s}$, respectively; $P = .023$). Postoperatively, the lesion's MD was also significantly lower than the nonlesioned cord on the contralateral side ($1.121 \pm 0.259 \times 10^{-3} \text{ mm}^2/\text{s}$; $P = .003$). The lesion's FA values ($0.406 \pm .69$) were significantly lower than the preoperative values of the normal cervical cord at the same segment (0.603 ± 0.145 ; $P = .001$) as well as the contralateral nonlesioned cord values on the postoperative scan (0.565 ± 0.130 ; $P = .001$).

Interestingly, patients with higher minimal MD values had improved postoperative BPI severity scores. The minimal MD correlated significantly with a greater relative decrease in the BPI severity score ($r = -0.821$, $P = .004$). A higher average MD showed a tendency toward similar trends, but results were not statistically significant ($r = -0.450$, $P = .192$). No significant association was demonstrated between either minimal, maximal, or average FA and changes in postoperative BPI severity ($r = -0.148$, $P = .688$; $r = 0.255$, $P = .476$; and $r = 0.292$, $P = .413$, respectively) (Table 1).

Lesion Parameters Over Time

Five patients were able to undergo a repeat MR imaging 1 month after surgery. The lesion volume on T2-weighted imaging significantly decreased from $0.25 \text{ cc} \pm 0.06 \text{ cc}$ on postoperative day 1 (POD 1) to $0.05 \text{ cc} \pm 0.02 \text{ cc}$ 1 month later ($P = .043$). The lesion volume on diffusion images decreased nonsignificantly, from $0.08 \text{ cc} \pm 0.04 \text{ cc}$ to $0.05 \text{ cc} \pm 0.03 \text{ cc}$ over 1 month ($P = .066$). However, the lesion's percentage of the cord's cross-sectional area on T2-weighted imaging and diffusion decreased significantly, from 21.5 ± 5.4 to 14.2 ± 3.2 ($P = .043$) and from 24.11 ± 12.77 to 13.19 ± 7.71 ($P = .043$), respectively.

The sagittal length (major axis) on T2-weighted imaging decreased significantly, from $12.8 \text{ mm} \pm 2.4 \text{ mm}$ on POD 1 to

Table 2: Imaging characteristics of patients with and without immediate postoperative contralateral pain

POD 1 Contralateral Pain	Yes 5/15	No 10/15	Sig.
Pain side, right, <i>n</i> (%)	2 (40%)	6 (60%)	.608
T2-weighted imaging total cord, %	17.46 ± 10.27	20.10 ± 7.91	.270
Diffusion, total cord, %	14.60 ± 7.60	15.67 ± 9.65	.999
MD	0.804 ± 0.98	1.019 ± 0.222	.037
FA	0.402 ± 0.07	0.408 ± 0.073	.903

Note:—Sig indicates significance.

8.8 mm ± 0.8 mm 1 month later ($P = .043$). The lesion's in-plane axial length (minor axis) on diffusion decreased significantly, from 5.2 ± 0.98 mm to 4.6 ± 1.0 mm ($P = .043$). We did not find any significant differences when we compared the lesion's sagittal length on diffusion or axial length on T2-weighted imaging between the POD 1 and the 1-month postoperative MRIs ($P = .08$ and $P = .08$, respectively). The MD showed a nonsignificant increase from 0.926 ± 0.251 to $1.070 \pm 0.285 \times 10^{-3}$ mm²/s; $P = .08$). We found no significant changes in FA from POD 1 to 1 month after surgery (0.409 ± 0.083 and 0.361 ± 0.063 , respectively; $P = .225$).

Contralateral Pain

Pain contralateral to the original one appeared immediately after surgery in 5 of the 15 patients (33%), which, with 1 exception, was considered less severe than the original one. We did not detect any significant differences between patients with and those without immediate postoperative contralateral pain in terms of lesion volume or percentage of the involved cord ($P = .270$ and $P = .999$ for T2-weighted imaging and DWI, respectively). The MD was significantly lower among patients with contralateral pain ($P = .037$), but the FA showed no significant association ($P = .903$) (Table 2).

Three patients in our cohort had clear preoperative documentation of metastatic lesions contralateral to the side of the originally painful lesion. All 3 had relief of their original pain, but 2 of them developed postoperative contralateral pain. Eight patients had lesions that were assumed to at least partially involve midline structures. However, because of their frailty, we were unable to obtain more recent adequate oncologic imaging data from all 15 patients.

One month after surgery, 9/14 (64%) reported developing contralateral pain, which was as severe as the original pain in 1 patient. Six of these 9 patients (66%) required medical treatment for relief of the contralateral pain. Of note, 8 of them had tumors along the midline or on the contralateral side that could be the cause of the new contralateral pain.

DISCUSSION

In this prospective study, we characterized the postoperative changes on MR imaging studies after percutaneous RF cordotomy. We further examined the correlations between postcordotomy diffusivity and T2 MR imaging changes and 2 clinical outcomes, pain improvement and the development of contralateral pain. In addition, we observed the evolution of the imaging characteristics of the ablated area up to 1 month from surgery. We hypothesize that postoperative parenchymal

imaging changes could reflect intraoperative events, and after correlating such changes to clinical results, we might therefore be able to search for ways to improve surgical technique and outcomes.

It has been previously shown that ablation of at least 20% of the cord is required to achieve optimal pain improvement after cordotomy.⁹ However, these

numbers derive from a histology-based cohort from the 1990s, and they were based on older surgical techniques that were associated with relatively lower success and safety profiles. That report was later challenged by a more contemporary series by Vedantam et al,¹⁰ who showed similar degrees of pain relief when comparing patients with ablations above and below 20% of the cord-cross sectional area, as represented by postoperative T2-weighted MR imaging. Similarly, our current study did not detect any significant differences in the decrease in NRS between patients with lesions below or above 20% of the cord's cross-sectional area based on both T2-weighted imaging and DWI. Lesions encompassing as low as 13% of the cord's cross-sectional area achieved excellent and long-term pain control. Therefore, our findings agree with the conclusions of Vedantam et al,¹⁰ who stated that larger lesions do not necessarily represent adequate ablation of the STT. In fact, we showed that smaller lesions on diffusion imaging correlated with greater improvement on the BPI severity score, probably signifying better intraoperative localization of the STT while sparing the need for repeated repositioning of the electrodes (Table 1, Fig 3). This is also explained by the fact that, as was previously shown and in accordance with our results, the size of the lesions on postcordotomy T2-weighted imaging directly correlates with the number of pial penetrations.¹⁰ We believe that more accurate localization of the STT, based on improved imaging and neurophysiologic techniques, may decrease the need for unnecessary repeated positioning of the electrodes and result in smaller surgical lesions and better pain control outcomes.

To our knowledge, this is the first study to describe the evolution of the imaging characteristics of cordotomy ablated areas up to 1 month after surgery. Our results showed that the lesions' percentage of the cord's cross-sectional areas on both T2-weighted imaging and diffusion imaging decreased significantly from POD1 to 1 month after surgery. Because only 5 patients were able to arrive for the scheduled 1-month postoperative MR imaging, we were not able to search for potential correlations between the lesions' dynamics and clinical outcomes at this point. We are currently gathering more data on this topic.

Furthermore, we analyzed the MD and FA values of the lesion on DTI. Whereas MD quantifies the diffusion of water molecules within tissues, FA estimates the degree of tissue organization. Overall, these parameters may indicate the degree of tissue injury, as was previously shown in patients after cordotomy and patients with spinal injuries.^{12,14-16}

Similar to previous reports, FA was significantly lower in the lesioned side of the cord compared with the nonlesioned side.¹² Our study also demonstrated a significant decrease in tissue FA of the targeted cervical cord area from pre- to postoperative DTI. FA values did not change at 1 month after surgery ($P = .225$).

Tissue FA decreased after neuronal tissue ablation because of disruption of axons that are aligned longitudinally, as was previously shown in studies of spinal cord injuries.^{17,18} Decreased FA has been associated with impaired white matter microstructure, including myelin damage, increased axonal diameter, low axonal attenuation, and impaired cellular membrane.^{19,20} In addition, we found significantly lower MD values in the lesioned area compared with the nonlesioned cord on the contralateral side. The lesion's MD was also significantly lower compared with the same area's MD on preoperative imaging. We then observed a non-significant increase in the lesion's MD at 1 month after surgery ($P = .08$). These results represent acute changes that typically follow sudden neural tissue insults, such as trauma or ischemic stroke.^{17,18,21} MD is initially decreased within the first few hours because of restriction of the movement of water molecules in the intracellular compartment. MD is later increased after the disruption of tissue barriers and the formation of necrotic tissue, but FA often stays decreased because of permanent axonal disruption.²¹

Interestingly, we found a significant correlation between the lesions' minimal MD values on postoperative scans and improved BPI severity scores after cordotomy. Average MD values showed a similar trend in relation to BPI severity, but the correlation was nonsignificant. No significant correlations were seen between FA values and changes in BPI after surgery. Our results are therefore in line with a previous study that found a correlation between the lesions' MD (but not FA) and the degree of improvement in the 1-week postoperative BPI severity score.¹² A higher MD is believed to be associated with cellular edema, demyelination, and disruption of membranes, which follow RF ablation.¹² Therefore, although MD values on immediate postoperative MR imaging are generally lower in the ablated area compared with nonlesioned tissue, higher MD values may, in fact, indicate better ablation of the neural tissue during cordotomy.

The development of contralateral pain after unilateral cordotomy has been reported in 17%–73% of patients.^{3,6–8} This type of pain is commonly reported as less severe when compared with the original one and is usually well controlled with pain medications. The mechanisms behind this phenomenon are still controversial because it is often difficult to differentiate between pure new-onset mirror pain and pain that is related to an underlying midline or contralateral disease. It is believed that pure mirror-image pain is a type of referred pain resulting from chronic changes in the spinal cord circuitry, coupled with disinhibition following ablation of descending pain inhibitory pathways.⁷ In our study, pain in the contralateral side appeared immediately after surgery in 33% of the cases and increased to 64% within 1 month after surgery. In most cases, this new pain was significantly less severe than the original one. We did not find any significant impact of the size of the lesion on the occurrence of immediate postoperative contralateral pain. However, patients who developed postoperative contralateral pain had lower MD on their immediate postoperative MR imaging.

Even though our patients were not asked to undergo preoperative total-body imaging, we assume that at least some of them harbored nonpainful metastatic lesions involving midline axial or contralateral structures. Previous reports emphasized the role of the dorsal columns in transmitting visceral and potentially also

midline axial pain. They mentioned the higher effectiveness of midline myelotomy (either thoracic or cervical) in eliminating midline pain compared with anterolateral cordotomy.^{22–24} It is therefore plausible that pain transmitted from silent midline spinal or pelvic tumors could potentially reach the surface after eliminating the more dominant original pain by unilateral cordotomy and contribute to the contralateral pain phenomenon. We plan to gather more preoperative total-body imaging data to investigate the correlation between the distribution of nonpainful metastatic spread, the ablation's anatomic characteristics, and the contralateral pain phenomenon.

Limitations

The main limitation of this study is its small cohort size. Additional correlations between different factors, including subgroup analyses, would have been possible with a larger patient population. Furthermore, pre- and 1-month postoperative BPI questionnaires were available for only 10/15 of the patients, mainly because of the medical and psychosocial complexity of our patients, as well as clinical deterioration and even death. Having more data derived from this well-validated tool would allow a better quantification of the studied associations.¹³ In addition, our imaging studies were performed within 24 hours after surgery. The patients' complex conditions made it too difficult to bring them back for a 1-month follow-up MR imaging study in parallel to the clinical evaluation. Therefore, we are currently working on increasing our data to analyze whether changes in diffusion MD values and the size of the lesions over time correlate with clinical outcomes.

CONCLUSIONS

The results of this study suggest that postoperative MR imaging has a role in predicting clinical outcomes after cordotomy. Even though a minimal size of ablation is required, larger lesions do not necessarily indicate better outcomes. Smaller lesions may signify better intraoperative localization of the spinothalamic tract and are correlated with better outcomes. Changes in MD and FA values represent neural tissue damage after ablation, and increased lesion MD values may be linked to better clinical response.

Disclosure: Ido Strauss—RELATED: Grant: European Society for Stereotactic and Functional Neurosurgery.* *Money paid to institution.

REFERENCES

1. Harsh V, Viswanathan A. **Surgical/radiological interventions for cancer pain.** *Curr Pain Headache Rep* 2013;17:331 [CrossRef Medline](#)
2. Raslan AM, Cetas JS, McCartney S, et al. **Destructive procedures for control of cancer pain: the case for cordotomy.** *J Neurosurg* 2011;114:155–70 [CrossRef Medline](#)
3. Strauss I, Berger A, Arad M, et al. **O-arm-guided percutaneous radiofrequency cordotomy.** *Stereotact Funct Neurosurg* 2017;95:409–16 [CrossRef Medline](#)
4. Raslan AM. **Percutaneous computed tomography-guided radiofrequency ablation of upper spinal cord pain pathways for cancer-related pain.** *Neurosurgery* 2008;62:226–33; discussion 233–34 [CrossRef Medline](#)
5. Kanpolat Y, Ugur HC, Ayten M, et al. **Computed tomography-guided percutaneous cordotomy for intractable pain in malignancy.** *Neurosurgery* 2009;64:ons187–93; discussion ons193–94 [CrossRef Medline](#)

6. Berger A, Hochberg U, Zegerman A, et al. **Neurosurgical ablative procedures for intractable cancer pain.** *J Neurosurg* 2019;1–8 [CrossRef](#)
7. Nagaro T, Adachi N, Tabo E, et al. **New pain following cordotomy: clinical features, mechanisms, and clinical importance.** *J Neurosurg* 2001;95:425–31 [CrossRef Medline](#)
8. Bain E, Hugel H, Sharma M. **Percutaneous cervical cordotomy for the management of pain from cancer: a prospective review of 45 cases.** *J Palliat Med* 2013;16:901–07 [CrossRef Medline](#)
9. Lahuerta J, Bowsher D, Lipton S, et al. **Percutaneous cervical cordotomy: a review of 181 operations on 146 patients with a study on the location of “pain fibers” in the C-2 spinal cord segment of 29 cases.** *J Neurosurg* 1994;80:975–85 [CrossRef Medline](#)
10. Vedantam A, Hou P, Chi TL, et al. **Postoperative MRI evaluation of a radiofrequency cordotomy lesion for intractable cancer pain.** *AJNR Am J Neuroradiol* 2017;38:835–39 [CrossRef Medline](#)
11. Vedantam A, Bruera E, Hess KR, et al. **Somatotomy and organization of spinothalamic tracts in the human cervical spinal cord.** *Neurosurgery* 2019;84:E311–17 [CrossRef Medline](#)
12. Vedantam A, Hou P, Chi TL, et al. **Use of spinal cord diffusion tensor imaging to quantify neural ablation and evaluate outcome after percutaneous cordotomy for intractable cancer pain.** *Stereotact Funct Neurosurg* 2017;95:34–39 [CrossRef Medline](#)
13. Bendinger T, Plunkett N. **Measurement in pain medicine.** *BJA Education* 2016;16:310–15 [CrossRef](#)
14. Vedantam A, Jirjis MB, Schmit BD, et al. **Diffusion tensor imaging of the spinal cord: insights from animal and human studies.** *Neurosurgery* 2014;74:1–8; discussion 8; quiz 8 [CrossRef Medline](#)
15. Martin AR, Aleksanderek I, Cohen-Adad J, et al. **Translating state-of-the-art spinal cord MRI techniques to clinical use: a systematic review of clinical studies utilizing DTI, MT, MWF, MRS, and fMRI.** *NeuroImage Clin* 2016;10:192–238 [CrossRef Medline](#)
16. Vedantam A, Eckardt G, Wang MC, et al. **Clinical correlates of high cervical fractional anisotropy in acute cervical spinal cord injury.** *World Neurosurg* 2015;83:824–28 [CrossRef Medline](#)
17. Shanmuganathan K, Gullapalli RP, Zhuo J, et al. **Diffusion tensor MR imaging in cervical spine trauma.** *AJNR Am J Neuroradiol* 2008;29:655–59 [CrossRef Medline](#)
18. Li XH, Li JB, He XJ, et al. **Timing of diffusion tensor imaging in the acute spinal cord injury of rats.** *Sci Rep* 2015;5:12639 [CrossRef Medline](#)
19. Sampaio-Baptista C, Johansen-Berg H. **White matter plasticity in the adult brain.** *Neuron* 2017;96:1239–51 [CrossRef Medline](#)
20. Takahashi M, Hackney DB, Zhang G, et al. **Magnetic resonance microimaging of intraaxonal water diffusion in live excised lam-prey spinal cord.** *Proc Natl Acad Sci U S A* 2002;99:16192–96 [CrossRef Medline](#)
21. Alegiani AC, MacLean S, Braass H, et al. **Dynamics of water diffusion changes in different tissue compartments from acute to chronic stroke—a serial diffusion tensor imaging study.** *Front Neurol* 2019;10:158 [CrossRef Medline](#)
22. Willis WD, Al-Chaer ED, Quast MJ, et al. **A visceral pain pathway in the dorsal column of the spinal cord.** *Proc Natl Acad Sci U S A* 1999;96:7675–79 [CrossRef Medline](#)
23. Nauta HJ, McIlwrath SL, Westlund KN. **Punctate midline myelotomy reduces pain responses in a rat model of lumbar spine pain: evidence that the postsynaptic dorsal column pathway conveys pain from the axial spine.** *Cureus* 2018;10:e2371 [CrossRef Medline](#)
24. Nauta HJ, Hewitt E, Westlund KN, et al. **Surgical interruption of a midline dorsal column visceral pain pathway. Case report and review of the literature.** *J Neurosurg* 1997;86:538–42 [CrossRef Medline](#)